Supporting information

$NiCo_2S_4$ octahedral configuration doped by Mn, Zn and Cu for oxygen evolution reaction

Yiting Chen[a,b], Hongyan Wu[a,c], Ning Tang[c], Yong Zhang[c,*] and Yuqiao Wang[a, b, *]

[a] Research Center for Nano Photoelectrochemistry and Devices, School of Chemistry and Chemical Engineering, Southeast University, Nanjing 211189, China

[b] Yangtze River Delta Carbon Neutrality Strategy Development Institute, Southeast University, Nanjing 210096, China

[c] College of Textile Science and Engineering (International Silk College), Zhejiang Sci-Tech University, Hangzhou 310018, China

[*] Corresponding author. Tel: +86 25 52090619; Fax: +86 25 52090621

E-mail address: zhangyong@zstu.edu.cn (Y. Zhang), yqwang@seu.edu.cn (Y. Wang).

Experimental Section

Chemicals

All chemical reagents were analytical grade and used directly without further purification. A piece of nickel foam (NF, 4 cm × 3 cm) was pretreated by 3 M HCl under sonication and washed by deionized water and alcohol three times, respectively.

Materials Synthesis

Synthesis of M-NiCo (M = Mn, Cu, Zn) precursor

Typically, 0.48 g $NiCl_2·6H_2O$, 0.95 g $CoCl_2·6H_2O$, 1.6 g hexamethylenetetramine, and 0.019 g $MnCl_2$ (0.026 g $CuCl_2·2H_2O$ or 0.021 g $ZnCl_2$) were added into 60 mL of deionized water under stirring for 30 min to form a transparent solution. The mole ratio of the doped element to the main elements is about 1:40. Then, the mixture was transferred into a 100 mL Teflon-lined stainless-steel autoclave with the clean NF at 100 °C for 8 h. The M-NiCo (M = Mn, Cu, Zn) precursor was gained after being washed with absolute ethanol three times to remove impurities and dried at 60 °C overnight in a vacuum.

Synthesis of M-$NiCo_2S_4$ (M = Mn, Cu, Zn) nanosheets

The homogeneous solution was prepared with 0.96 g $Na_2S·9H_2O$ dissolved in 60 mL of deionized water under stirring for 30 min to form a transparent solution. The solution was transferred into a 100 mL Teflon autoclave with an as-prepared M-NiCo (M = Mn, Cu, Zn) precursor and maintained at 160 °C for 5 h. M-$NiCo_2S_4$ (M = Mn, Cu, Zn) was obtained after being washed with absolute ethanol three times to remove impurities and dried at 60 °C overnight in a vacuum.

For comparison, $NiCo_2S_4$ was synthesized by the same method. The loading masses of $NiCo_2S_4$, Mn-$NiCo_2S_4$, Cu-$NiCo_2S_4$ and Zn-$NiCo_2S_4$ were of 1.26, 3.17, 2.00 and 1.49 mg cm^{-2}, respectively.

Materials Characterizations

The morphologies and structures were characterized by scanning electron microscope (SEM,

FEI Inspect F50), transmission electron microscope (TEM) and high-resolution TEM (HRTEM, FEI TECNAI G2 20) with the energy dispersive spectrometer mapping analysis. The crystal structure was analyzed by X-ray diffraction (XRD, Ultima IV). The X-ray photoelectron spectroscopy (XPS, AXIS Ultra) was used to detect surface bonding.

Electrochemical Measurements

All electrochemical measurements were carried out on the electrochemical workstation (CHI 760E) in 1.0 M KOH. The OER performance was recorded using a three-electron system with a graphite rod as a counter electrode and a standard calomel electrode (SCE) as a reference electrode.

Linear sweep voltammetry (LSV) curves were collected at a scan rate of 2 mV s^{-1} with 90% iR compensation. We applied the negative scanning direction to avoid the influence of oxidation peak on overpotential in the LSV measurement. Tafel slopes were obtained from the curves of the overpotential versus the logarithm of current density according to LSV curves. All potentials were converted to a reversible hydrogen electrode (RHE) using the equation: $E_{RHE} = E_{SCE} + 0.241\ V + 0.059 \times pH$. The C_{dl} values were evaluated based on cyclic voltammetry (CV) curves under non-Faradaic region. Electrochemical active surface area (ECSA) was calculated as following equation: $ECSA = C_{dl} / C_s$, C_s means a general specific capacitance (0.04 mF cm^{-2}). Electrochemical impedance spectroscopy (EIS) was monitored with an amplitude of 5 mV and the frequency range from 10 kHz to 0.01 Hz. The multicurrent processes and chronopotentiometry curve were investigated without iR compensation.

For comparison, the RuO_2 and Ni foam were evaluated. The working electrodes of RuO_2 was prepared by dispersing 2 mg powders into a water–ethanol solution containing 10 μL Nafion and sonicating for 1 h to form a homogeneous catalyst ink. Then the catalyst ink was cast onto Ni foam and dried in air at room temperature.

Mn-$NiCo_2S_4$ as anode and the commercial Pt/C as cathode, the water splitting performance was tested. The preparation of Pt/C electrode is similar to that of RuO_2. Linear sweep voltammetry (LSV) curves were collected at a scan rate of 2 mV s^{-1} and stability tests were performed at the current density of 10 mA cm^{-2}. As a comparison, the water splitting performance of RuO_2 as anode and Pt/C as cathode was also evaluated.

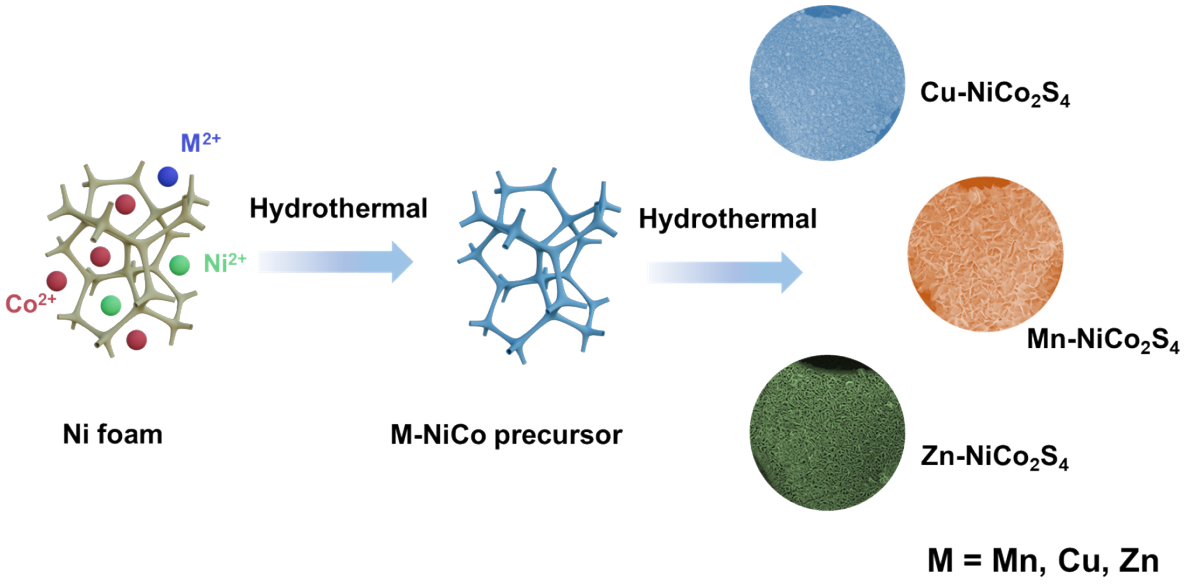

Fig. S1. Schematic illustration for the synthesis of M-$NiCo_2S_4$ (M = Mn, Cu, Zn).

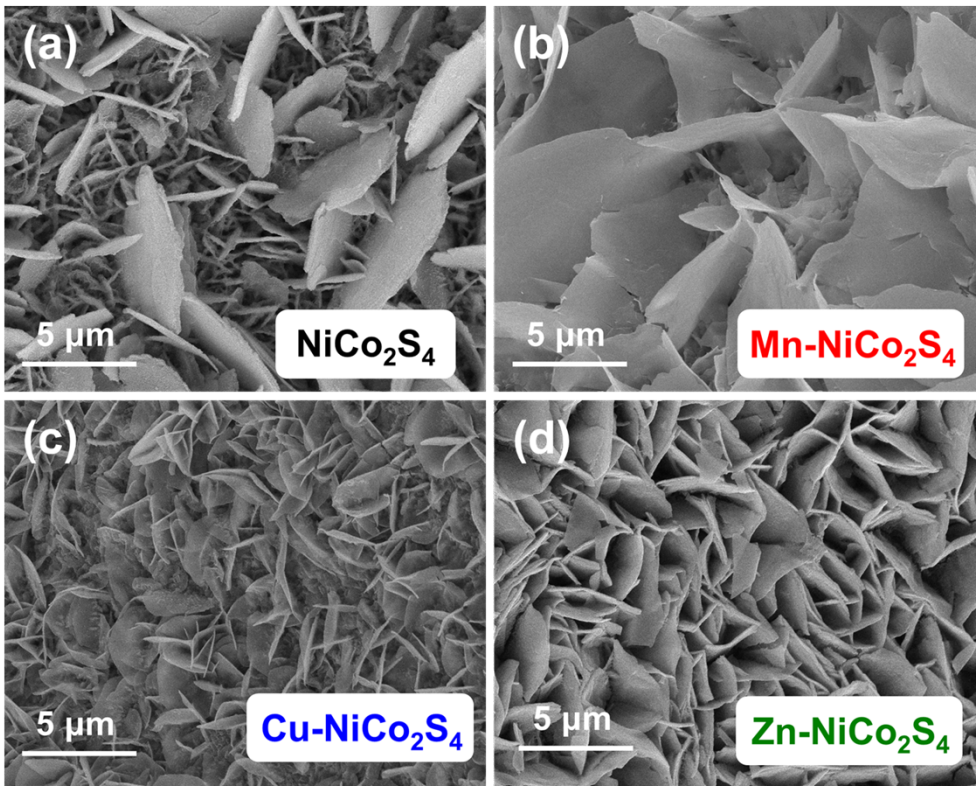

Fig. S2. SEM images of (a) $NiCo_2S_4$, (b) Mn-$NiCo_2S_4$, (c) Cu-$NiCo_2S_4$, (d) Zn-$NiCo_2S_4$.

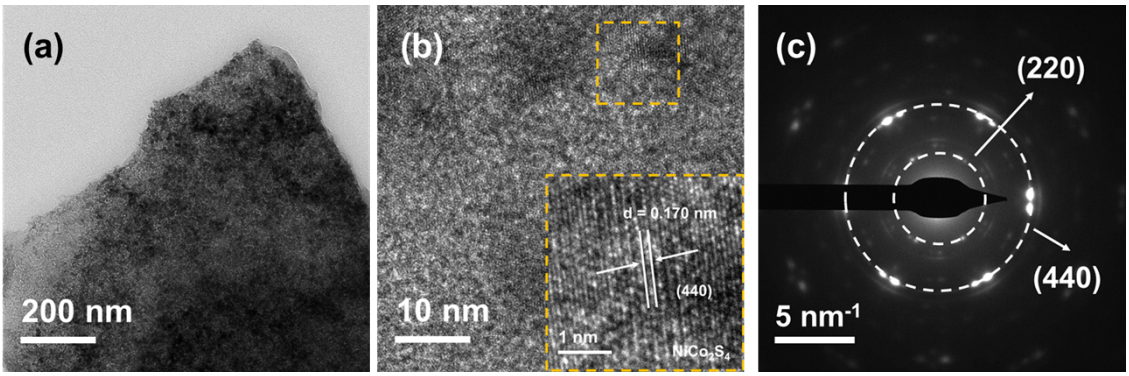

Fig. S3. (a) TEM, (b) HRTEM image and (c) Electron diffraction pattern of $NiCo_2S_4$.

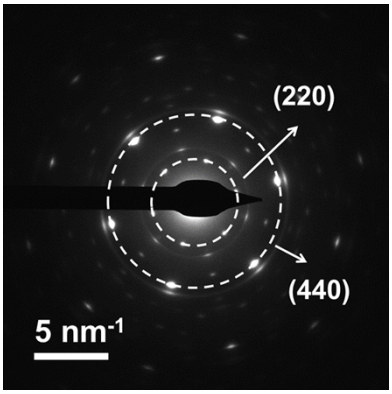

Fig. S4. Electron diffraction pattern of Mn-$NiCo_2S_4$.

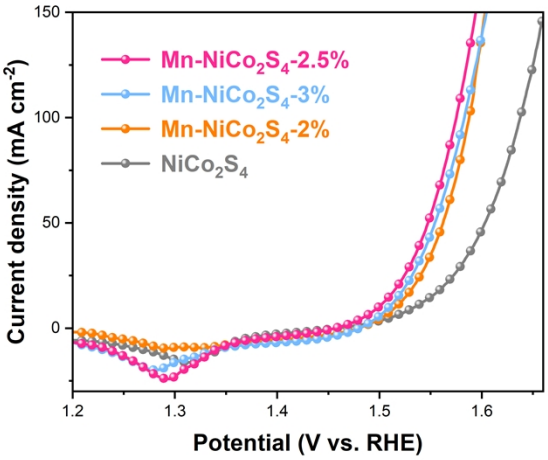

Fig. S5. LSV curves of Mn-$NiCo_2S_4$ with different doping amount.

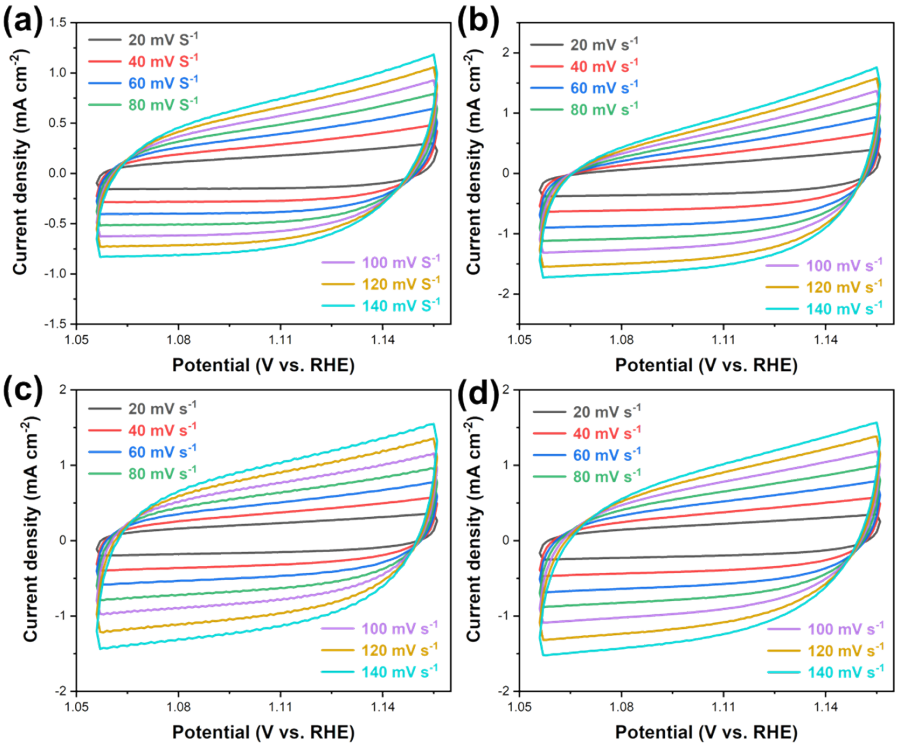

Fig. S6. CV curves of (a) $NiCo_2S_4$, (b) Mn-$NiCo_2S_4$, (c) Cu-$NiCo_2S_4$, (d) Zn-$NiCo_2S_4$.

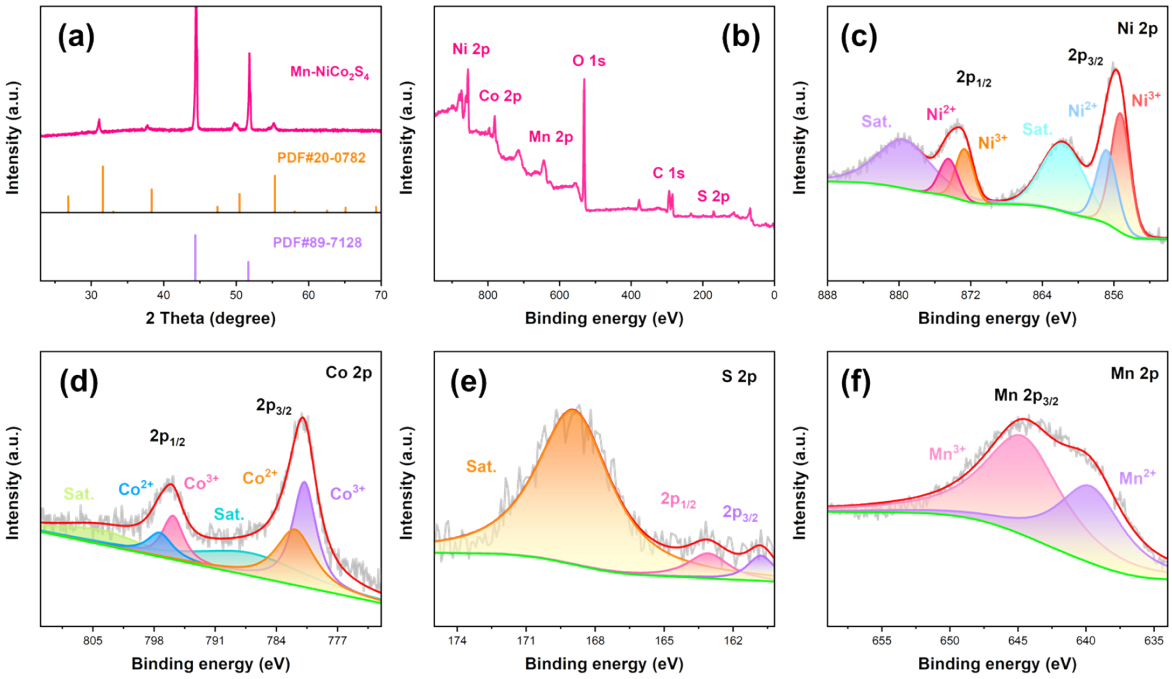

Fig. S7. (a) XRD and (b-f) XPS patterns of Mn-$NiCo_2S_4$ after chronoamperometric (i-t) curves.

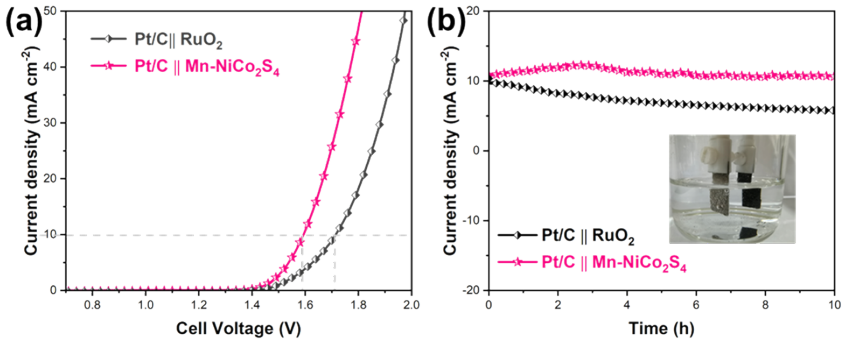

Figure S8. (a) Linear sweep voltammetry (LSV) curves and (b) Chronoamperometric (i-t) curves of Pt/C||RuO_2 and Pt/C||Mn-$NiCo_2S_4$ electrodes (inset: bubble image of Pt/C||Mn-$NiCo_2S_4$ electrodes).

Table S1. Atomic ratio (%) of doping elements in M-$NiCo_2S_4$ by XPS analysis

Elements	M-$NiCo_2S_4$ (M = Mn, Cu, Zn)
Mn	3.68
Cu	3.26
Zn	3.30

Table S2. The corresponding EIS parameters of the as-prepared $NiCo_2S_4$, Zn-$NiCo_2S_4$, Mn-$NiCo_2S_4$ and Cu-$NiCo_2S_4$ catalysts.

	$NiCo_2S_4$	Zn-$NiCo_2S_4$	Mn-$NiCo_2S_4$	Cu-$NiCo_2S_4$
R_s (ohm)	2.45	2.31	1.70	2.27
R_1 (ohm)	4.51	2.15	0.51	0.76
R_2 (ohm)	6.60	3.93	3.21	3.52
CPE1-T	2.30	0.41	0.87	0.61
CPEI-P	0.64	0.73	0.56	0.71
CPE2-T	2.07	0.54	1.11	0.52
CPE2-P	0.92	0.97	0.86	0.93

Table S3. Comparison of OER performance between the catalyst prepared in this work with other electrocatalysts in 1 M KOH.

Catalysts	OER performance		References
	Overpotential (mV)	Tafel slope (mV dec^{-1})	
Mn-$NiCo_2S_4$	269	55.4	This work
$NiCo_2S_4$@NiCoNC/CC	280	81.8	[1]
Ni/Co_9S_8@CNT	289	69.0	[2]
Co_9S_8-ZnS/NTC	290	69.0	[3]
CoS-Ag	293	55.3	[4]
Fe–Co_9S_8@CoO	296	65.0	[5]
MoS_2/$NiPS_3$	296	86.0	[6]
Ni_3S_2-QDs/SNC	310	73.0	[7]
Ni-1T-MoS_2	310	103.2	[8]
FeCo-3/NSC	312	96.4	[9]
$MnCo_2S_4$	317	73.7	[10]
$Ni(OH)_2$/MoS_2 NFs	328	69.3	[11]
Co/Co_9S_8/MnS-NMC	330	55.1	[12]
Mn-CoN_x/N-PC	330	136.0	[13]
Co_9S_8/MnS-USNC	360	137.0	[14]
$NiCo_2S_4$/RGO	366	65.0	[15]

Table S4. Comparison of water splitting performance between the catalyst prepared in this work with other electrocatalysts in 1 M KOH.

anode	cathode	cell voltage(V) for OWS	References
Mn-$NiCo_2S_4$/NF	Pt/C	1.59	This work
$MnCo_2S_4$/NF	$MnCo_2S_4$/NF	1.61	[16]
NiS/NF	NiS/NF	1.64	[17]
$NiCo_2S_4$ NA/CC	$NiCo_2S_4$ NA/CC	1.68	[18]
a-NiO	a-NiO	1.70	[19]
Fe, S-CoP	Pt/C	1.59	[20]
CoO@Cu_2S	Pt/C	1.60	[21]
NiFeP/MXene	Pt/C	1.61	[22]

References

1 Z. Wang, L. Yang, S. Liu, H. Yu, X. Li, Y, Xu, L. Wang and H. Wang, *Nanotechnology*, 2020, **31**, 195402

2 X. Hu, W. Wang, B. Liang, D. Sun, Y. Gao, W. Liao, Q. Yang, G. Li and X. Zuo, *Catal. Lett.*, 2021, **152**, 1321-1330

3 Y. Yang, D. Wang, Y. Wang, Z. Li, R. Su, X. Wang, T. Xu and S. Wang, *ACS Appl. Energy Mater.*, 2022, **5**, 14869-14880

4 S. Cheng, R. Zhang, W. Zhu, W. Ke and E. Li, *Appl. Surf. Sci.*, 2020, **518**, 146106

5 T. Wang, C. Li, X. Liao, Q. Li W. Hu, Y. Chen, W. Yuan and H. Lin, *Int. J. Hydrogen. Energ.*, 2022, **47**, 21182-21190

6 Y. Liu, Y. Chen, Y. Tian, T. Sakthivel, H. Liu, S. Guo, H. Zeng and Z. Dai, *Adv. Mater.*, 2022, **34**, 2203615

7 F. Xu, J. Wang, Y. Zhang, W. Wang, T. Guan, N. Wang and K. Li, *Chem. Eng. J.*, 2022, **432**, 134256

8 G. Wang, G. Zhang, X. Ke, X. Chen, X. Chen, Y. Wang, G. Huang, J. Dong, S. Chu and M. Sui, *Small*, 2022, **18**, 2107238

9 S. Chang, H. Zhang and Z. Zhang, *J. Energy Chem.*, 2021, **56**, 64-71

10 Z. Dai, X. Feng, Q. Li, P. Su, X. Shen, Y. Zheng, Q. Jiao, Y. Zhao, H. Li and C. Feng, *J. Alloy Compd.*, 2021, **872**, 159652

11 K. T. Le, N. N. T. Pham, Y. S. Liao, A. Ranjan, H. Y. Lin, P. H. Chen, H. Nguyen, M. Y. Lu, S. G. Lee and J. M. Wu, *J. Mater. Chem. A*, 2023, **11**, 3481-3492

12 K. Chen, X. Wang, C. Zhang, R. Xu, H. Wang, L. Chu, M. Huang, *Mater Toady Energy*, 2022,

30, 101150

13 H. Zheng, F. Ma, H. Yang, X. Wu, R. Wang, D. Jia, Z. Wang, N. Lu, S. Peng and F. Ran, *Nano Research*, 2022, **15**, 1942-1948

14 J. Li, W. Li, H. Mi, Y. Li, L. Deng, Q. Zhang, C. He and X. Ren, *J. Mater. Chem. A*, 2021, **9**, 22635-22642

15 C. Shuai, Z. Mo, X. Niu, X. Yang, G. Liu, J. Wang, N. Liu and R. Guo, *J. Mater. Sci.*, 2020, **55**, 1627-1636

16 B. Hou, J. Fu, H. Su and X. Du, *Chem. Select*, 2019, **4**, 4499-4505

17 W. Zhu, X. Yue, W. Zhang, S. Yu, Y. Zhang, J. Wang and J. Wang, *Chem. Commun.*, 2016, **52**, 1486-1489

18 D. Liu, Q. Lu, Y. Luo, X. Sun and A. M. Asiri, *Nanoscale*, 2015, **7**, 15122-15126

19 X. Zhang and X. Du, *New J. Chem.*, 2020, **44**, 1703-1706

20 L. Tian, X. Pang, H. Xu, D. Liu, X. Lu, J. Li, J. Wang and Z. Li, *Inorg. Chem.*, 2022, **61**, 16944-16951

21 Y. Li, X. Zhang, S. Zhuo, S. Liu, A. Han, L. Li and Y. Tian, *Appl.Surf. Sci.*, 2021, **555**, 149441

22 J. Chen, Q. Long, K. Xiao, T. Ouyang, N. Li, S. Ye and Z.-Q. Liu, *Sci. Bull.*, 2021, **66**, 1063-1072